^{68}Ga-Siderophores for PET Imaging of Invasive Pulmonary Aspergillosis: Proof of Principle

Milos Petrik[1], Hubertus Haas[2], Georg Dobrozemsky[1], Cornelia Lass-Flörl[3], Anna Helbok[1], Michael Blatzer[2], Hermann Dietrich[4], and Clemens Decristoforo[1]

[1]Clinical Department of Nuclear Medicine, Innsbruck Medical University, Innsbruck, Austria; [2]Department of Molecular Biology, Innsbruck Medical University, Innsbruck, Austria; [3]Department of Hygiene, Microbiology and Social Medicine, Innsbruck Medical University, Innsbruck, Austria; and [4]Laboratory Animal Facilities, Innsbruck Medical University, Innsbruck, Austria

The diagnosis of invasive pulmonary aspergillosis (IPA) is difficult and lacks specificity and sensitivity. In the pathophysiology of *Aspergillus fumigatus*, iron plays an essential role as a nutrient during infection. *A. fumigatus* uses a specific and highly efficient iron uptake mechanism based on iron-complexing ferric ion Fe(III) siderophores, which are a requirement for *A. fumigatus* virulence. We aimed to evaluate the potential of siderophores radiolabeled with ^{68}Ga, a positron emitter with complexing properties comparable to those of Fe(III), as a radiopharmaceutical for imaging IPA. **Methods:** ^{68}Ga radiolabeling of the *A. fumigatus* siderophores desferri-triacetylfusarinine C (TAFC) and desferri-ferricrocin (FC) was performed at high specific activity. Stability, protein binding, and log P values were determined. In vitro uptake in *A. fumigatus* cultures was tested under varying conditions. Biodistribution was studied in healthy noninfected BALB/c mice, and uptake was studied in a model of *A. fumigatus* infection using immunosuppressed Lewis rats. **Results:** High-specific-activity ^{68}Ga labeling could be achieved, and resulting complexes were stable in serum, toward diethylenetriaminepentaacetic acid and Fe(III) challenge. Both siderophores showed hydrophilic properties (^{68}Ga-TAFC, log P = −2.59; ^{68}Ga-FC, log P = −3.17) with low values of protein binding for ^{68}Ga-TAFC (<2%). Uptake of both siderophores was highly dependent on the mycelial iron load and could be blocked with an excess (10 μM) of siderophore or NaN_3, indicating specific, energy-dependent uptake. In noninfected mice, ^{68}Ga-TAFC showed rapid renal excretion and low blood values (1.6 ± 0.37 percentage injected dose per gram [%ID/g] at 30 min); in urine only intact ^{68}Ga-TAFC was detected. In contrast, ^{68}Ga-FC revealed high retention in blood (16.1 ± 1.07 %ID/g at 90 min) and rapid metabolism. In the rat IPA model, lung uptake of ^{68}Ga-TAFC was dependent on the severity of infection, with less than 0.04 %ID/g in control rats (n = 5) and 0.29 ± 0.11 %ID/g in mildly infected (n = 3) and 0.95 ± 0.37 %ID/g in severely infected (n = 4) rats. PET showed focal accumulation in infected lung tissue. **Conclusion:** Both siderophores bound ^{68}Ga with high affinity, and ^{68}Ga-TAFC, especially, showed high stability. ^{68}Ga-TAFC displayed highly selective accumulation by *A. fumigatus* subspecies in vitro and in vivo. The high and specific uptake by *A. fumigatus* proves the potential of ^{68}Ga-labeled siderophores for the specific detection of *A. fumigatus* during infection. They hold promise as new PET agents for IPA.

Key Words: invasive pulmonary aspergillosis; fungal infection; siderophores; ^{68}Ga; PET

J Nucl Med 2010; 51:639–645
DOI: 10.2967/jnumed.109.072462

Aspergillus subspecies, especially *A. fumigatus*, are among the most common airborne fungi. With an expanding population of immunosuppressed patients, the incidence of severe and often fatal invasive pulmonary aspergillosis (IPA), mainly caused by *A. fumigatus,* has increased tremendously during the past decades and is currently the most common mold infection worldwide (*1,2*). IPA is now a major direct or contributory cause of death in leukemia patients and a common cause of compromised chemotherapy and failure of remission-induction chemotherapy. It is a major cause of mortality among bone marrow and stem cell transplant recipients (*3*). Typically, mortality associated with this disease reaches 50%−100%, one of the major reasons being current limitations in diagnosis.

Early diagnosis is critical to a favorable outcome of IPA but is difficult to achieve with currently available diagnostic tools; for example, of 314 invasive fungal infections in patients with hematologic malignancies, 75% were not diagnosed antemortem (*4*). Newer antifungal agents exhibit differential mold activity, thus increasing the importance of establishing a specific diagnosis of IPA. A range of alternate diagnostic strategies is currently being used (*5*), including radiology, CT, cultures, and several serologic tests. Also, scintigraphic techniques have been proposed including ^{67}Ga-citrate and, rarely, ^{18}F-FDG PET. None of these techniques, however, has shown sufficient sensitivity and specificity for

Received Nov. 5, 2009; revision accepted Jan. 5, 2010.
For correspondence or reprints contact: Clemens Decristoforo, Clinical Department of Nuclear Medicine, Innsbruck Medical University, Anichstrasse 35, A-6020 Innsbruck; Austria.
E-mail: Clemens.Decristoforo@uki.at

allowing the early detection of IPA, with subsequent optimal treatment of patients.

It has recently been recognized that iron plays an essential role in infection in general (*6*) and in IPA in particular. Haas et al. (*7*), Schrettl et al. (*8*), and Wallner et al. (*9*) reported that *A. fumigatus* produces siderophores (low-molecular-mass chelators with high affinity for ferric ions (*10*)) for iron acquisition and storage, respectively, and uses highly efficient siderophore transporters for uptake of iron (*11*). Mutational inactivation of the siderophore biosynthesis system (*12*) impairs the virulence of this pathogen. The absolute essentiality of the siderophore system for virulence of *A. fumigatus* concomitantly with upregulation of genes encoding siderophore biosynthetic enzymes and siderophore transporters in a murine model for IPA demonstrates that the siderophore system is activated during pathogenic growth (*13*).

The main siderophores produced by *A. fumigatus* are desferri-triacetylfusarinine C (TAFC) and desferri-ferricrocin (FC) (*8*), which both display exceptional high affinity for ferric ions Fe(III) with picomolar values of 31.8 and 25.6, respectively, and have the ability to remove iron from transferrin (*14*). TAFC is a cyclic tripeptide consisting of 3 N^2-acetyl-N^5-*cis*-anhydromevalonyl-N^5-hydroxyornithine residues linked by ester bonds, and FC is a cyclic hexapeptide with the structure Gly-Ser-Gly-(N^5-acetyl-N^5-hydroxyornithine)$_3$ (Fig. 1) (*15*). Because ^{68}Ga has a chemistry comparable to Fe(III), we aimed to evaluate the potential of these siderophores radiolabeled with ^{68}Ga for PET of IPA. Here we describe the radiolabeling with ^{68}Ga and preclinical evaluation of TAFC and FC including evaluation of ^{68}Ga-TAFC–mediated imaging in a rat IPA model.

MATERIALS AND METHODS

Reagents

All chemicals obtained commercially were of analytic grade and used without further purification. TAFC and FC were obtained from Genaxxon Bioscience GmbH.

Fungal Strains and Growth Conditions

The studies were performed with *A. fumigatus* strain 46645 (American Type Culture Collection) cultured at 37°C in *Aspergillus* minimal medium as previously described (*16*). The pH was adjusted to 6.5. Iron-replete medium was made by adding $FeSO_4$ to a final concentration of 30 μM (iron-supplemented). For iron-depleted conditions, addition of iron was omitted (iron-deficient). Iron starvation was verified by the detection of TAFC production, which is repressed by iron.

Labeling

^{68}Ga was obtained from a ^{68}Ge/^{68}Ga generator (IGG; Eckert & Ziegler), eluted with 0.1N HCl (biochemical grade; Fluka). To various amounts of FC and TAFC (1–30 nmol) dissolved in water (~500 μM), 30 μL of sodium acetate solution (1.1 M in water) and 300 μL of the generator eluate (10–100 MBq of $^{68}GaCl_3$) were added. After 10 min at room temperature, 100 μL of sodium acetate solution were added to increase the pH to 6–7. The radiochemical purity of the radiolabeled siderophore was analyzed on reversed-phase high-performance liquid chromatography (HPLC) (TAFC retention time = 17.1 min; FC retention time = 12.1 min).

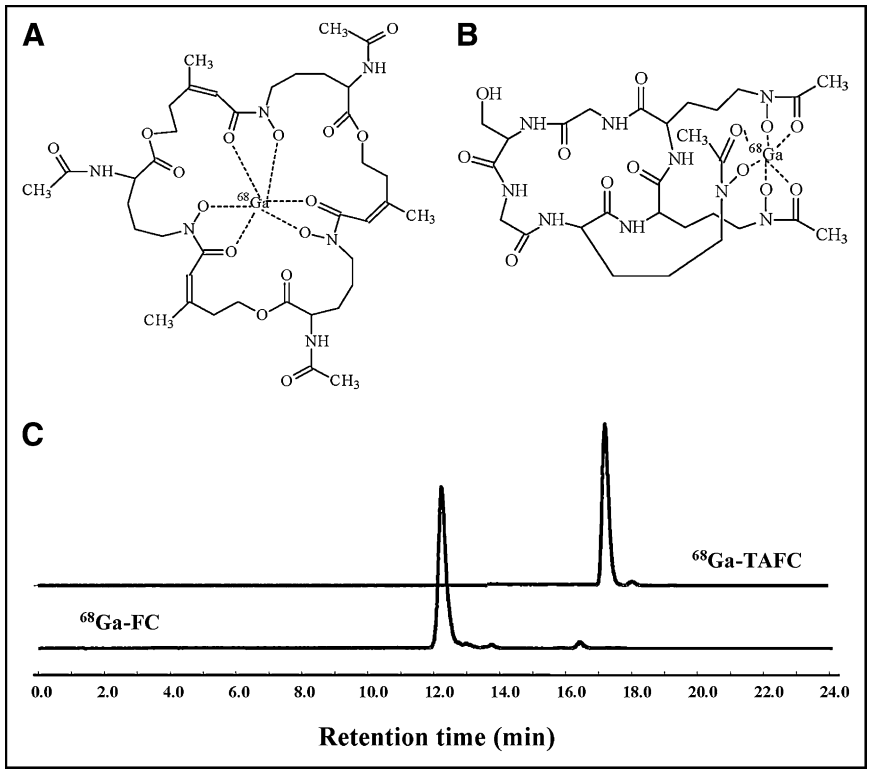

FIGURE 1. Proposed chemical structures of ^{68}Ga-TAFC (molecular weight, 919.64 g/mol) (A) and ^{68}Ga-FC (molecular weight, 784.43 g/mol) (B), and HPLC-radiochromatograms (RP-C18, ACN/H_2O/0.1% trifluoroacetic acid gradient) of ^{68}Ga-TAFC and ^{68}Ga-FC 10 min after incubation of 100 MBq of ^{68}Ga with 10–15 nmol of TAFC or FC at pH 3.9 (C).

HPLC

A P680 HPLC pump with a UVD 170 U ultraviolet/visible spectra detector (Dionex) and a Bioscan radiometric detector (Bioscan) were used for reversed-phase HPLC analysis. A Nucleosil 120-5 C18 250 × 4.6 mm column (Bischoff), with flow rates of 1 mL/min and ultraviolet detection at 220 and 254 nm, was used with the following gradient: acetonitrile (ACN)/0.1% trifluoroacetic acid/H_2O: 0–2 min, 0% ACN; 2–15 min, 0%−36% ACN; 15–18 min, 36%−60% ACN; 18–19.5 min, 60% ACN; 19.5–20 min, 60%−0% ACN; and 20–24 min, 0% ACN.

Log P, Protein Binding, and Stability (Serum, Diethylenetriaminepentaacetic Acid [DTPA], Iron-Containing Solution)

Stability. ^{68}Ga-labeled FC and TAFC were incubated in human serum, DTPA solution (6 mM), and 0.1 M $FeCl_3$ solution for 30, 60, and 120 min, respectively, at 37°C. Subsequently, serum was mixed with ethanol, and after centrifugation the supernatant was injected onto the HPLC column. Samples from mixtures containing DTPA and $FeCl_3$ were analyzed directly.

Log P. To 0.5 mL of the radiolabeled siderophore in phosphate-buffered saline, 0.5 mL of octanol in a microcentrifuge tube was added. The tube was stirred vigorously in a vortex mixer over a period of 15 min. An aliquot of the aqueous and the octanol layer was collected and then counted in the γ-counter (Compugamma; LKB Wallac), and log P values were calculated (mean of $n = 6$).

Protein Binding. ^{68}Ga-labeled TAFC or FC was incubated in fresh human serum at 37°C and analyzed after 30, 60, and 120 min by size-exclusion chromatography (MicroSpin G-50 or Sephadex G-50 columns; GE Healthcare). Protein binding of the radiolabeled siderophores was determined by measuring the activity on the column and the activity in the eluate using a γ-counter.

Uptake Assays

For the monitoring of uptake over time, ^{68}Ga-labeled siderophore was incubated with iron-deficient or iron-supplemented *A. fumigatus* for 10, 20, 30, 45, 60, and 90 min at room temperature with or without blocking solution (Fe-TAFC or Fe-FC) in 96-well filter plates (Millipore). Incubation was interrupted by filtration of the medium and rapid rinsing with ice-cold Tris buffer, and filters were counted in a γ-counter.

For the uptake assays, ^{68}Ga-labeled siderophores were incubated with iron-supplemented or iron-deficient *A. fumigatus* for 45 min at room temperature with and without sodium azide or excess of either Fe(III) or siderophore. Incubation was interrupted by filtration of the medium and rapid rinsing with ice-cold Tris buffer, and filters were counted in a γ-counter.

Release Assays

^{68}Ga-labeled siderophores were incubated with iron-deficient *A. fumigatus* for 1 h (uptake). Cultures were centrifuged and washed twice with phosphate-buffered saline. Cultures were incubated at room temperature in phosphate-buffered saline with or without blocking solution (Fe-TAFC or Fe-FC) in 6-well plates (Greiner Bio-One). During incubation, 500 μL samples were taken at different times (15, 30, 45, 60, and 90 min) and centrifuged. In a γ-counter, 300 μL samples of supernatant and total cultures were counted. Release was expressed as percentage of total uptake in total cultures.

Animal Experiments

All animal experiments were conducted in accordance with regulations of the Austrian Animal Protection Laws and with the approval of the Austrian Ministry of Science (66011/42-II/10b/2009). Animal studies were performed using BALB/c mice and Lewis rats (Charles River Laboratories).

Biodistribution in Noninfected Mice

A group of 6 mice (females, 6 wk old) received ^{68}Ga-labeled siderophore (2 MBq/mouse, corresponding to 0.1–0.3 nmol of siderophore) injected into the tail vein. Mice were sacrificed by cervical dislocation 30 and 90 min after injection ($n = 3$ at each time). Different organs and tissues (blood, lungs, heart, stomach, spleen, liver, pancreas, kidneys, muscle, intestines, and bone) were removed. The amount of radioactivity was determined with a γ-counter. Results were expressed as percentage of injected dose per gram of tissue.

Rat IPA Model

In vivo imaging studies were performed in Lewis rats (female, 2–3 mo old), adapting a published IPA model (*17*). Profound neutropenia was induced by a single intraperitoneal administration of 75 mg of cyclophosphamide per kilogram (Endoxan; Baxter Oncology GmbH) 5 d, followed by a 75 mg/kg dose of cyclophosphamide 1 d before *A. fumigatus* inoculation. To prevent bacterial superinfections, animals were given 35 mg of teicoplanin per kilogram (Targocid; Sanofi-Aventis GmbH) intramuscularly 5 d before *A. fumigatus* inoculation, followed by 25 mg/kg doses of teicoplanin 1 d before and on the day of inoculation. In addition, rats received 2 mM ciprofloxacin (Fresenius Kabi GmbH) and 100 μM polymyxin E (Colistin; Grünenthal GmbH) in their drinking water throughout the experiment. Fungal infection was established by the intratracheal application of 150–250 μL of *A. fumigatus* in various concentrations (10^5−10^8 colony-forming units [CFU]/mL). On the day of the experiment (3 d after inoculation), rats received the radioactive siderophore (~20 MBq/rat, corresponding to 1–3 nmol of siderophore) injected into the femoral vein. Rats were sacrificed by overdosing with ketamine:xylazine (2:1; Schoeller Chemie) 2 h after injection. Different organs and tissues (blood, lungs, spleen, liver, and kidneys) were removed. The amount of radioactivity was determined with a γ-counter. Results were expressed as percentage of injected dose per gram of tissue (%ID/g). *A. fumigatus* infection was confirmed in cultures of the excised organs. Tissue specimens were homogenized aseptically and investigated for fungi by culture (CFU count) and microscopic examination using Fungi-Fluor (Calcofluor White staining solution; Polysciences). Severe infection was defined as detection of CFUs 1 d after incubation, mild infection was defined as no detection of CFUs before day 3 of incubation, and no infection was defined as lack of fungal growth within 1 wk of incubation. The control group was treated equivalently but was not subjected to *A. fumigatus* inoculation.

^{68}Ga-TAFC Imaging in Rat IPA Model

Lewis rats were anesthetized by intramuscular application of Ketasol (ketamine; 80–100 mg/kg of body weight [BW]) and Xylasol (xylazine; 5–10 mg/kg of BW). ^{68}Ga-TAFC solutions were injected intravenously into the left femoral vein in a maximum volume of 0.3 mL, with a total activity of 50–100 MBq/kg of BW corresponding to 5–10 μg of siderophore per kilogram of BW. Imaging was performed with a clinical PET scanner (Advance; GE Healthcare) in anterior prone position starting

5 min after the injection of ^{68}Ga-TAFC with 3 sets of a static emission image of 20-min duration, immediately followed by an acquisition for attenuation correction lasting 10 min.

Reconstruction was performed using the ordered-subset expectation maximization algorithm with attenuation correction and model-based scatter correction. The reconstruction settings were 2 iterations and 28 subsets to a 128 × 128 matrix, with a transaxial field of view of 12.8 cm, interupdate of 1.0 mm, and postfiltering of 1.4 mm. The resulting in-plane voxel size was 1.0 mm, and the plane thickness was 4.25 mm. Transmission data were reconstructed into a matrix of equal size by means of filtered backprojection, yielding a coregistered image set. The reconstructed emission images were reformatted into coronal, sagittal, and maximum-intensity-projection image sets.

Statistical Analysis

The in vivo biodistribution data of rats were compared using 1-way ANOVA, followed by Tukey's honestly significant differences post hoc test for 3 or more independent samples (level of significance, $P < 0.05$). Analysis was performed using SPSS, version 15.0.1 (SPSS, Inc.), for Windows (Microsoft).

RESULTS

Radiolabeling and In Vitro Characterization

High-specific-activity labeling was achieved using both TAFC and FC at pH 3.9 using acetate buffer. However, quantitative labeling using 100 MBq of ^{68}Ga was observed with less than 1 nmol of TAFC, whereas for FC more than 15 nmol were required. Figure 1 shows chemical structures and radiochromatograms of ^{68}Ga-TAFC and ^{68}Ga-FC, with a single main peak for both ^{68}Ga-labeled siderophores. In particular, ^{68}Ga-TAFC complexes were extremely stable in solution, showing no degradation in serum even after 2 h of incubation and no release of ^{68}Ga even when challenged with Fe(III) or DTPA. For ^{68}Ga-FC, some release (<20%) was observed toward challenge with Fe(III). Both ^{68}Ga-TAFC and ^{68}Ga-FC siderophores showed hydrophilic properties (^{68}Ga-TAFC, log P = −2.59; ^{68}Ga-FC, log P = −3.17), with low protein binding for ^{68}Ga-TAFC (<2%) but more than 50% for FC (30–90 min of incubation).

In Vitro Uptake and Release Studies

Uptake by *A. fumigatus* of both ^{68}Ga-TAFC and ^{68}Ga-FC was highly dependent on the mycelial iron load: iron-starved but not iron-replete mycelia displayed high uptake that could be blocked with an excess (10 μM) of cold iron siderophore or NaN_3, indicating a specific, energy-dependent uptake mechanism (Fig. 2); nonspecific accumulation was considerably higher for ^{68}Ga-FC. Uptake was observed up to 90 min after incubation without saturation, again sensitive to specific blocking and dependent on the mycelial iron load for both ^{68}Ga-labeled siderophores.

In a release assay, ^{68}Ga-siderophores showed high retention in *A. fumigatus* over a period of more than 2 h. However, when coincubated with an excess of cold iron siderophore, significant release of ^{68}Ga-FC was observed whereas ^{68}Ga-TAFC remained trapped (Supplemental Fig. 1; supplemental materials are available online only at http://jnm.snmjournals.org).

Biodistribution and Metabolism in Noninfected BALB/c Mice

In noninfected mice (Fig. 3), ^{68}Ga-TAFC showed rapid renal excretion and low blood levels, even at short times after injection (1.6 ± 0.37 %ID/g; 30 min); in urine, only intact ^{68}Ga-TAFC was detected. In contrast, FC revealed a high retention in blood (16.1 ± 1.07 %ID/g; 90 min) and organs, indicating rapid metabolism with no detection of intact ^{68}Ga-labeled siderophore excreted renally.

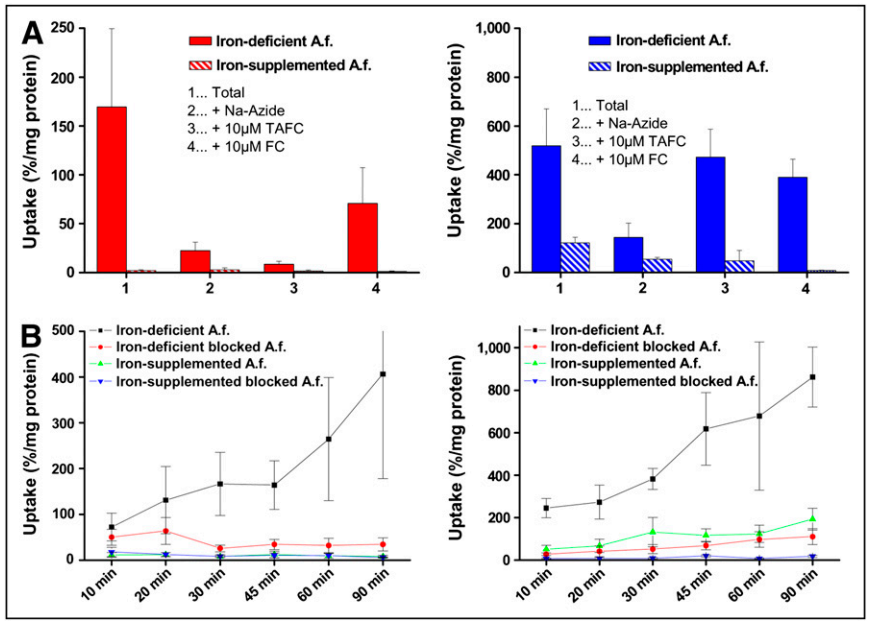

FIGURE 2. Uptake studies of ^{68}Ga-labeled siderophores (TAFC, left; FC, right). (A) Uptake in *A. fumigatus* after 45 min of incubation under varying conditions: 2 mM sodium azide, 10 μM excess iron siderophores in both iron-supplemented and iron-deficient conditions. (B) Uptake over time under iron-supplemented and iron-deficient conditions and in presence of 10 μM excess siderophore (blocking). A.f. = *A. fumigatus*.

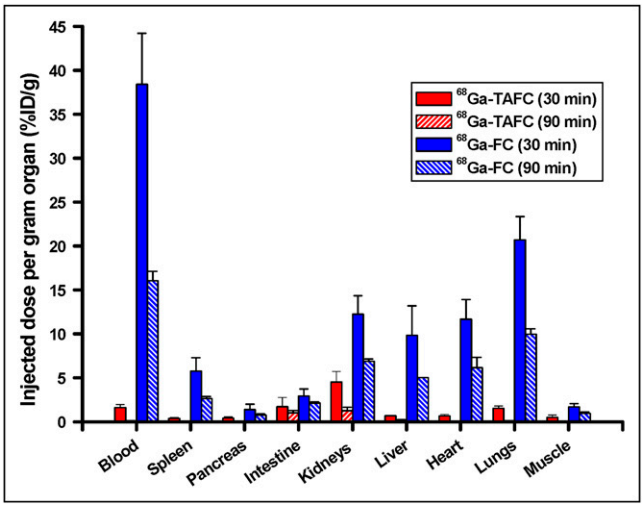

FIGURE 3. Biodistribution of ^{68}Ga-TAFC and ^{68}Ga-FC in noninfected BALB/c mice 30 and 90 min after injection.

Biodistribution of ^{68}Ga-TAFC in Rat IPA Model

Of 11 infected rats, 4 developed a severe lung infection, 3 developed a mild infection, and 4 showed no sign of infection at all. Severely infected animals also revealed mild infection in other organs such as kidneys and liver, whereas in the other groups no other organ infection could be detected. No significant difference in organ uptake between the infected and the noninfected groups, except for lung uptake, was observed. Figure 4 summarizes lung uptake values in the different groups of rats. Highest uptake of ^{68}Ga-TAFC was observed in severely infected rats, with 0.95 ± 0.37 %ID/g (n = 4), followed by 0.29 ± 0.11 %ID/g (n = 3) in mildly infected animals. The group showing no infection (negative, 0.036 ± 0.007 %ID/g) and the control group (0.039 ± 0.011 %ID/g) showed comparable uptake, with no significant difference; uptake in these groups was significantly lower than that in infected rats ($P < 0.05$).

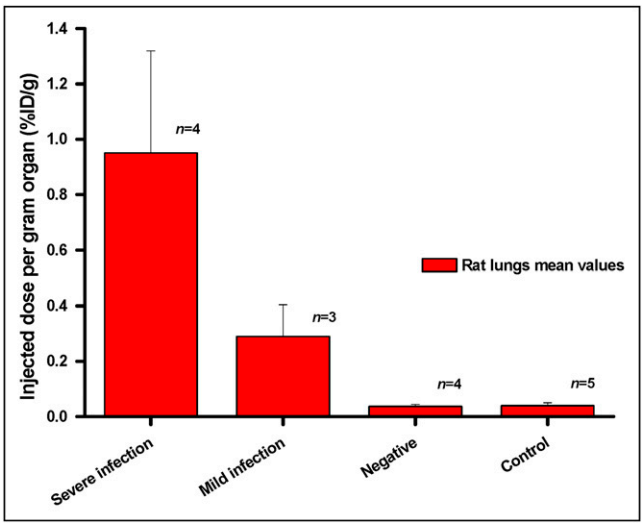

FIGURE 4. Lung uptake of ^{68}Ga-TAFC in infected vs. noninfected rats. Negative = rats inoculated with *A. fumigatus* but negative in postmortem tissue cultures.

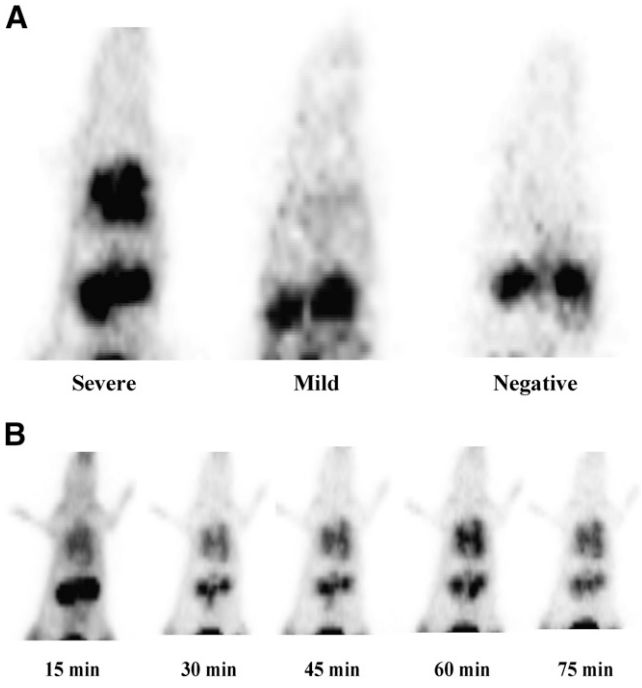

FIGURE 5. (A) PET in rat IPA model showed accumulation of ^{68}Ga-TAFC in infected lung tissue, dependent on severity of infection. (B) Dynamic imaging showed rapid uptake and no release of ^{68}Ga-TAFC over time in infected lungs.

Imaging

PET of severely infected rats revealed rapid uptake of ^{68}Ga-TAFC in infected lungs, accompanied by rapid renal elimination (Fig. 5). Already by 15 min after injection, a high contrast between lungs and surrounding tissue was observed, improving at 30 min and then remaining constant for the whole imaging period of 75 min. No washout from lung tissue could be measured, and the only visible organs besides lungs were the kidneys. Faint lung uptake was detected in a mildly infected rat, whereas in a control animal no uptake in the lung region was observed and the only organs visible were the kidneys. Highest activity concentrations were found in the bladder, increasing over time, whereas after initial peaking kidney activity remained constant.

DISCUSSION

In view of the high clinical need for improved diagnostic tools for imaging IPA, various attempts were made to develop suitable radiopharmaceuticals for this application, including ^{99m}Tc-labeled polyethyleneglycol-liposomes or ^{99m}Tc-interleukin 8 (*18*). Although some preclinical results were promising, the mechanism of uptake was not specific for fungal infections and clinical data are missing. Potentially more specific agents such as radiolabeled antifungal agents

(^{99m}Tc-fluconazole) or ^{99m}Tc-antimicrobial peptides (e.g., ubiquicidin) have been shown to be suboptimal for the detection of fungal infections and have never found their way into clinical trials (*19*).

Siderophore-based compounds, including deferoxamine, have been investigated in radiopharmaceutical research already in the early 1980s (*20,21*). ^{67}Ga is an isosteric diamagnetic substitute for Fe(III) (*22*), and thus, the affinity constants of many siderophores for gallium are in the range of their iron counterparts (*23*). Emery and Hoffer (*23*) have used ^{67}Ga to study the uptake mechanisms for different siderophores in *Ustilago sphaerogena* and found this energy-dependent process to be indistinguishable from that of the Fe(III) counterpart. They even postulated an involvement of siderophore binding in the accumulation of ^{67}Ga-citrate in inflammatory lesions. However, only recently has the importance of iron metabolism and acquisition in the pathophysiology of infection been fully recognized (*6*). Iron plays an essential role in the immunocompetence of the host, because of effects on immune cells and its interference with cell-mediated immune effector pathways and cytokine activities. At the same time, iron is crucial for the proliferation of pathogens including *A. fumigatus,* because of its essential role in numerous pathways (*15*). Part of the infection process can, therefore, be regarded as a battle for iron between host and pathogen. To succeed in this battle, *A. fumigatus* produces 2 main siderophores, FC and TAFC, together with highly efficient siderophore transporters. Therefore, we attempted to use the same siderophores radiolabeled with ^{68}Ga as Trojan horses to allow specific imaging of the infection process. The use of the generator-based radionuclide ^{68}Ga provides the basis for immediate availability for rapid diagnostic answers, and PET guarantees the highest diagnostic sensitivity and resolution currently available in nuclear medicine. High specificity for fungal infections can be expected, as the siderophores TAFC and FC have no function in the human physiology. Rapid accumulation based on the highly efficient siderophore transporter system appears advantageous in comparison to, for example, cell wall–labeling approaches.

Here, we report the proof of principle for the detection of *A. fumigatus* by ^{68}Ga-TAFC. TAFC could be labeled with ^{68}Ga at high specific activities, and the resulting complex displayed excellent in vitro stability, which was confirmed in vivo by murine biodistribution studies showing no degradation products of ^{68}Ga-TAFC in urine. In contrast, ^{68}Ga-FC was considerably more unstable both in vitro and in vivo. Both siderophores were taken up by *A. fumigatus* cultures in an energy-dependent and saturable manner by iron-starved but not iron-replete cells, consistent with the expression pattern of *A. fumigatus* siderophore transporters (*11*). In contrast to ^{68}Ga-TAFC, ^{68}Ga-FC displayed unspecific binding and release of ^{68}Ga when the culture was subjected to an excess of siderophore, indicating inhibition of reuptake due to blocking of siderophore transporters. Additionally, biodistribution properties of ^{68}Ga-TAFC in mice were clearly superior to those of ^{68}Ga-FC. This finding is in accordance with the specific role of these 2 siderophores for *A. fumigatus*: TAFC is used for extracellular iron acquisition, whereas FC is predominantly used for intracellular storage and transport. In a rat IPA model, uptake of ^{68}Ga-TAFC in lungs was clearly correlated with the severity of the infection. This confirms that *A. fumigatus* remains in an iron-starved status during infection as shown previously (*13*). Nontarget activity was rapidly eliminated by the kidneys, and activity in the lungs showed high retention—retention for up to 2 h after injection—providing high target-to-nontarget ratios over the whole image acquisition period of 2 h. This holds promise to allow imaging over a prolonged time.

An important clinical need is to identify fungal infections early after the onset of disease and to discriminate different pathogens. *A. fumigatus* accounts for more than 90% of all IPAs; other *Aspergillus* subspecies, therefore, play a minor role. On the other hand, there is no indication of any difference in siderophore uptake between *Aspergillus* subspecies. Bacterial species have not been shown to use Fe-TAFC, and Fe-TAFC uptake by *Candida albicans* is inefficient (*24*), which holds promise that ^{68}Ga TAFC may be a selective compound for the detection of IPA. Furthermore, sensitive detection of *Aspergillus* infections in other organs besides the lung is of high clinical relevance. The generally low background activity enables infection detection in other areas such as the brain, with the exception of the kidneys, where in general small peptides show intense and prolonged nonspecific retention.

Recently (*25*), the in vivo detection of IPA based on a hyphae-binding peptide (c(CGGRLGPFC)-NH_2) identified by phage display technology and labeled with ^{111}In has been reported. This study confirms the possibility of the direct detection of IPA in vivo. However, we believe that this approach has the disadvantage that targeting is based on extracellular binding without active, energy-mediated uptake and accumulation. The use of ^{111}In as a suboptimal radionuclide remains an additional challenge for this latter approach. Moreover, considering lower target uptake (0.37 ± 0.06 %ID/g vs. 0.95 ± 0.37 %ID/g for ^{68}Ga-TAFC) and higher background activity (0.14 ± 0.02 %ID/g vs. 0.027 ± 0.008 %ID/g for ^{68}Ga-TAFC), ^{68}Ga-TAFC appears to better suited for the imaging of IPA.

CONCLUSION

We have shown that the *A. fumigatus* siderophores FC and TAFC bind ^{68}Ga with high affinity and that ^{68}Ga-TAFC, especially, displays high stability in biologic systems. ^{68}Ga-TAFC revealed a highly selective accumulation by *A. fumigatus* both in vitro and in vivo, proving the potential of ^{68}Ga-labeled siderophores for specific infection imaging. Thus, ^{68}Ga-siderophores represent promising new PET agents for IPA, demanding further investigations to characterize the sensitivity and pathogen selectivity but also toxicity of these imaging compounds.

ACKNOWLEDGMENTS

We thank the staff of the Central Laboratory Animal Facilities for the continuous support in taking care of our animals, and we especially thank Sandra Leitner for providing cultures and performing tissue analysis. This work was supported by the Austrian Science Foundation (FWF) grant L676-B18 and partly by grant P18606-B11.

REFERENCES

1. Latge JP. Aspergillus fumigatus and aspergillosis. *Clin Microbiol Rev.* 1999;12:310–350.
2. Tekaia F, Latge JP. Aspergillus fumigatus: saprophyte or pathogen? *Curr Opin Microbiol.* 2005;8:385–392.
3. Kontoyiannis DP, Bodey GP. Invasive Aspergillosis in 2002: an update. *Eur J Clin Microbiol Infect Dis.* 2002;21:161–172.
4. Chamilos G, Luna M, Lewis RE, et al. Invasive fungal infections in patients with hematologic malignancies in a tertiary care cancer center: an autopsy study over a 15-year period (1989–2003). *Haematologica.* 2006;91:986–989.
5. Hope WW, Walsh TJ, Denning DW. Laboratory diagnosis of invasive aspergillosis. *Lancet Infect Dis.* 2005;5:609–622.
6. Weiss G. Iron and immunity: a double-edged sword. *Eur J Clin Invest.* 2002;32(suppl 1):70–78.
7. Haas H. Molecular genetics of fungal siderophore biosynthesis and uptake: the role of siderophores in iron uptake and storage. *Appl Microbiol Biotechnol.* 2003;62:316–330.
8. Schrettl M, Bignell E, Kragl C, et al. Distinct roles for intra- and extracellular siderophores during Aspergillus fumigatus infection. *PLoS Pathog.* 2007;3:1195–1207.
9. Wallner A, Blatzer M, Schrettl M, et al. Ferricrocin, a siderophore involved in intra- and transcellular iron distribution in Aspergillus fumigatus. *Appl Environ Microbiol.* 2009;75:4194–4196.
10. Drechsel H, Jung G. Peptide siderophores. *J Pept Sci.* 1998;4:147–181.
11. Schrettl M, Kim HS, Eisendle M, et al. SreA-mediated iron regulation in Aspergillus fumigatus. *Mol Microbiol.* 2008;70:27–43.
12. Schrettl M, Bignell E, Kragl C, et al. Siderophore biosynthesis but not reductive iron assimilation is essential for Aspergillus fumigatus virulence. *J Exp Med.* 2004;200:1213–1219.
13. McDonagh A, Fedorova ND, Crabtree J, et al. Sub-telomere directed gene expression during initiation of invasive aspergillosis. *PLoS Pathog.* 2008;4:e1000154.
14. Hissen AH, Moore MM. Site-specific rate constants for iron acquisition from transferrin by the Aspergillus fumigatus siderophores N′,N″,N‴-triacetylfusarinine C and ferricrocin. *J Biol Inorg Chem.* 2005;10:211–220.
15. Haas H, Eisendle M, Turgeon GS. Siderophores in fungal physiology and virulence. *Annu Rev Phytopathol.* 2008;46:149–187.
16. Pontecorvo G, Roper JA, Hemmons LM, et al. The genetics of Aspergillus nidulans. *Adv Genet.* 1953;5:141–238.
17. van Vianen W, de Marie S, ten Kate MT, et al. Caspofungin: antifungal activity in vitro, pharmacokinetics, and effects on fungal load and animal survival in neutropenic rats with invasive pulmonary aspergillosis. *J Antimicrob Chemother.* 2006;57:732–740.
18. Boerman OC, Dams ETM, Oyen WJG, et al. Radiopharmaceuticals for scintigraphic imaging of infection and inflammation. *Inflamm Res.* 2001;50:55–64.
19. Lupetti A, Welling MM, Pauwels EK, et al. Detection of fungal infections using radiolabeled antifungal agents. *Curr Drug Targets.* 2005;6:945–954.
20. Yokoyama A, Ohmomo Y, Horiuchi K, et al. Deferoxamine, a promising bifunctional chelating agent for labeling proteins with gallium: Ga-67 DF-HAS—concise communication. *J Nucl Med.* 1982;23:909–914.
21. Moerlein SM, Welch MJ, Raymond KN, et al. Tricatecholamide analogs of enterobactin as gallium- and indium-binding radiopharmaceuticals. *J Nucl Med.* 1981;22:710–719.
22. Llinas M, Klein MP, Neilands JB. Solution conformation of ferrichromes a microbial iron transport cyclohexapeptide, as deduced by high resolution proton magnetic resonance. *J Mol Biol.* 1970;52:399–414.
23. Emery T, Hoffer PB. Siderophore-mediated mechanism of gallium uptake demonstrated in the microorganism Ustilago sphaerogena. *J Nucl Med.* 1980;21:935–939.
24. Lesuisse E, Knight SAB, Camadro JM, et al. Siderophore uptake by Candida albicans: effect of serum treatment and comparison with Saccharomyces cerevisiae. *Yeast.* 2002;19:329–340.
25. Yang Z, Kontoyiannis DP, Wen X, et al. Gamma scintigraphy imaging of murine invasive pulmonary aspergillosis with a ^{111}In-labeled cyclic peptide. *Nucl Med Biol.* 2009;36:259–266.

JNM The Journal of NUCLEAR MEDICINE

^{68}Ga-Siderophores for PET Imaging of Invasive Pulmonary Aspergillosis: Proof of Principle

Milos Petrik, Hubertus Haas, Georg Dobrozemsky, Cornelia Lass-Flörl, Anna Helbok, Michael Blatzer, Hermann Dietrich and Clemens Decristoforo

J Nucl Med. 2010;51:639-645.
Doi: 10.2967/jnumed.109.072462

The Journal of Nuclear Medicine is published monthly.
SNMMI | Society of Nuclear Medicine and Molecular Imaging
1850 Samuel Morse Drive, Reston, VA 20190.
(Print ISSN: 0161-5505, Online ISSN: 2159-662X)

SNMMI SOCIETY OF NUCLEAR MEDICINE AND MOLECULAR IMAGING